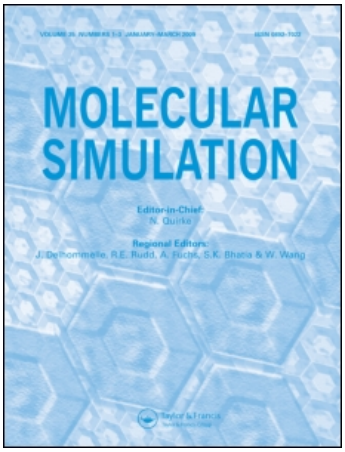

Molecular Simulation
Publication details, including instructions for authors and subscription information:
http://www.informaworld.com/smpp/title~content=t713644482

Water-Carbon Interactions 2: Calibration of Potentials using Contact Angle Data for Different Interaction Models

Richard L. Jaffe[a]; Pedro Gonnet[b]; Thomas Werder[b]; Jens H. Walther[b]; Petros Koumoutsakos[b]
[a] NASA Ames Research Center, Moffett Field, CA, USA [b] Institute of Computational Science, ETH Zurich, Zurich, Switzerland

To cite this Article Jaffe, Richard L. , Gonnet, Pedro , Werder, Thomas , Walther, Jens H. and Koumoutsakos, Petros(2004) 'Water-Carbon Interactions 2: Calibration of Potentials using Contact Angle Data for Different Interaction Models', Molecular Simulation, 30: 4, 205 — 216
To link to this Article: DOI: 10.1080/08927020310001659124
URL: http://dx.doi.org/10.1080/08927020310001659124

Molecular Simulation, VOL. 30 (4), 15 April 2004, pp. 205–216

Taylor & Francis
Taylor & Francis Group

Water–Carbon Interactions 2: Calibration of Potentials using Contact Angle Data for Different Interaction Models

RICHARD L. JAFFE[a,*], PEDRO GONNET[b], THOMAS WERDER[b], JENS H. WALTHER[b] and PETROS KOUMOUTSAKOS[b]

[a]*NASA Ames Research Center, Moffett Field, CA 94035, USA;* [b]*Institute of Computational Science, ETH Zurich, CH-8092 Zurich, Switzerland*

(Received July 2003; In final form October 2003)

Molecular dynamics simulations of water droplets on graphite are carried out to determine the contact angle for different water–carbon potential functions. Following the procedure of Werder *et al.* [*J. Phys. Chem. B*, 107 (2003) 1345], the C–O Lennard–Jones well depth is varied to recover the experimental value for the contact angle (84–86°) using a 2000-molecule water droplet and compensating for the line tension effect that lowers the contact angle for increasing droplet size. For the discrete graphite surface model studied by Werder *et al.*, the effects of adding C–H Lennard–Jones interactions and changing the long-range cut-off distance are considered. In addition, a continuum graphite surface model is studied for which the water–graphite interaction energy depends only on the normal distance (z) from the water oxygen to the surface. This new model, with z^{-10} repulsion and z^{-4} attraction, is formulated in terms of the standard Lennard–Jones parameters, for which the recommended values are $\sigma_{CO} = 3.19$ Å and $\varepsilon_{CO} = 0.3651$ kJ/mol.

Keywords: Graphite; Molecular dynamics; Contact angle; Water–graphite interface; Water–carbon potential functions

INTRODUCTION

As part of the recent fascination with nanotechnology, there has been considerable interest in designing, characterizing and fabricating nanoscale fluid flow devices for sensor applications. Single walled carbon nanotubes (SWNT) are one of the critical materials used for these sensors when a hydrophobic surface is required. Nanotubes are chosen because they are grown as tubules with diameter of 1–5 nm, have extremely high mechanical strength and excellent thermal and chemical stability. Functionalized carbon nanotubes (CNT) are being studied for use as nanoscale biosensors [1,2] and water or ion channels [3–5]. Several molecular dynamics (MD) studies of water in carbon nanotubes have recently been performed to gain further insight into the latter, but in these MD studies a wide range of intermolecular potentials for water and water–carbon interactions have been employed (see Ref. [6] for details). To date, the use of quantum chemistry calculations for determining the strength of the water–carbon surface interaction has not been successful. Calculations [7] of water–aromatic molecule interactions overestimate the magnitude of this quantity and accurate calculations for water molecules physisorbed on a graphene sheet using periodic boundary conditions are not feasible at this time. In addition, experimental data are not available for calibrating the strength of the water–carbon interaction, so it is difficult to assess the accuracy of these potentials.

In a recent study by Werder *et al.* [6] (paper 1 of this series, denoted subsequently as WWJHK), MD simulations were used to compute the static contact angle for nanometer-size water droplets on graphite and compared the results with available experimental data (86° by Fowkes [8] as cited in Ref. [9]; 84° by Morcos [10]; and 42° ± 7° by Schrader [11]). By matching the computed and measured contact angles, they were able to calibrate the C–O interaction strength parameter in their model potential for the water–carbon system. Using MD simulations, WWJHK found

*Corresponding author. E-mail: rjaffe@mail.arc.nasa.gov

ISSN 0892-7022 print/ISSN 1029-0435 online © 2004 Taylor & Francis Ltd
DOI: 10.1080/08927020310001659124

the value for the contact angle of a water droplet on graphite to vary inversely with the computed magnitude of the binding energy of a single water molecule to the graphite surface. They also found this binding energy, and the total water–carbon interaction energy per unit area of the droplet footprint, to vary linearly with the well-depth parameter of the pairwise Lennard–Jones potential used to model the water–carbon interaction. Therefore, the water–carbon well depth in the potential energy function could be chosen so the MD simulations would match any target value for the contact angle. Because the contact angle arises from a balance between water–water and water–graphite interaction strengths, this calibration is sensitive to the water model and other parameters used in the simulations. These include the cut-off distance for truncating long-range forces and other parameters used in describing the water–graphite interaction. In the present paper, we extend this analysis to alternative forms for the model potential. As was done by WWJHK, the higher experimental value for the contact angle (84–86°) is adapted for our calibration. However, an alternate calibration based on the smaller value (42° ± 7°) is also presented.

For the original study, the water–water interaction was described by the SPC/E [12] model, which uses rigid water molecules. The SPC/E intermolecular potential is given by a Lennard–Jones (12–6) interaction between oxygen atoms and coulomb interactions between partial electronic charges on the H and O atoms. A Lennard–Jones function between all pairs of water O-atoms and graphite carbons was used to compute the water–graphite interaction energy. The optimal Lennard–Jones well-depth (ε_{CO}) was found to be 0.392 kJ/mol. In the present study, we examine the effect of adding pairwise water hydrogen–graphite carbon Lennard–Jones terms and the effect of changing the long-range cut-off used in the truncation of the interactions. We also consider a continuum model of the graphite surface in which the interaction energy depends only on the normal distance from each water oxygen to the surface. The continuum model reduces the computational effort needed to determine the water surface interaction and also changes the nature of the long-range truncation of the water–carbon potential.

In the Second Section, the water–carbon potential models used to describe water–carbon surface interactions in recent published MD simulation studies are surveyed along with the continuum model developed for the present study. In the Third Section, the computational methodology is described and the results of the MD simulations are given in the Fourth Section. Our conclusions are presented in the Fifth Section.

WATER–CARBON POTENTIAL MODELS

In the studies published to date for MD simulations of the interface between liquid water and graphite or carbon nanotubes, the carbon surface–water interaction is usually described by atom–atom Lennard–Jones potentials between the C–O and (sometimes) the C–H pairs:

$$V_{CO} = \sum_i 4\varepsilon_{CO}\left[(\sigma_{CO}/R_i)^{12} - (\sigma_{CO}/R_i)^6\right], \quad (1)$$

where the index i runs over all pairs of C and O atoms and R_i is the distance between atoms in the ith pair. The well depth and position of the minimum in the potential are given by ε_{CO} and $(2^{1/6})\sigma_{CO}$, respectively (σ_{CO}, the separation where $V_{CO} = 0$, is also referred to as the sum of van der Waals radii of the C and O atoms). Often, the parameters for these potentials are based on standard Lorentz–Berthelot mixing rules:

$$\varepsilon_{CO} = (\varepsilon_{CC} \times \varepsilon_{OO})^{1/2} \quad \sigma_{CO} = (\sigma_{CC} + \sigma_{OO})/2 \quad (2)$$

which make them more dependent on the choice of C–C and O–O potentials than on the physical characteristics of the interface under study. It has been demonstrated for alkane melts, however, that more accurate results are obtained if independent values are chosen for these parameters [13].

Unfortunately, there is a paucity of experimental data that can be used for parameterization of these Lennard–Jones parameters. Qualitatively, it has been observed that water does not wet a graphite surface, but surface defects and impurities, such as oils from vacuum pumps or handling, as well as salts and absorbed gases in the water might inhibit wetting. Similarly, it is well known that carbon nanotubes are not soluble in water [14], indicating a fairly weak water–carbon interaction. Bojan and Steele [15] used experimental isotherm data for the physisorption of O_2 on porous carbon surfaces to determine the C–O parameters. For the gas phase water–benzene complex, the experimental binding energy [16] is −10.2 kJ/mol while the best quantum chemistry value [17] is −12.13 kJ/mol (−16.32 kJ/mol dissociation energy with a 4.18 kJ/mol correction for zero-point vibration energy). High-level quantum chemistry calculations of water–graphene interactions yield binding energies for a single water molecule of −24 kJ/mol [7]. If the C–O potential is calibrated to match this quantum chemistry result, MD simulations predict that water will wet the graphite surface [18]. In fact, the calibration study of WWJHK showed that complete wetting occurs if the magnitude of the water–graphite binding energy is greater than 12.8 kJ/mol (using the SPC/E water model and a pairwise C–O Lennard–Jones potential with a long-range cut-off of 10 Å). Thus, matching the experimental contact angle

may be the best method for calibrating potential functions for water–carbon interactions.

The WWJHK study determined the value of the Lennard–Jones parameter ε_{CO} that would enable a MD simulation to reproduce the macroscopic contact angle of 86° for a water droplet on graphite. In that work, the effect of droplet size on contact angle (θ) was taken into account by the use of the modified Young's equation:

$$\gamma_{SV} = \gamma_{SL} + \gamma_{LV}\cos\theta + \tau/r_B \quad (3)$$

where γ is the surface tension between two phases (with subscripts S, L and V indicating solid, liquid and vapor phase, respectively), τ is the line tension and r_B is the radius of the droplet at its interface with the surface. The footprint of the droplet on the surface is assumed to be circular. Equation (3) can be rearranged as

$$\cos\theta = \cos\theta_\infty - \tau/(\gamma_{LV} r_B) \quad (4)$$

where θ_∞ is the macroscopic contact angle (for $r_B \to \infty$). From consideration of droplets comprised of 1000 to 17576 water molecules, the line tension was found to be $2\text{–}3 \times 10^{-10}$ J/m, in agreement with a recent experimental determination by Mugele *et al.* [19] for sub-micron size droplets. For the standard 2000-water molecule droplets used in the calibration, the contact angle correction due to droplet size ($\cos\theta - \cos\theta_\infty$) is 8°. WWJHK determined that using $\varepsilon_{CO} = 0.392$ kJ/mol will result in a contact angle of 95.3°, which corresponds, to a macroscopic contact angle of 87°.

Table I contains a summary of the potentials used to date for water–graphite and water–carbon nanotube interactions. The potentials used by Markovic [20], Gordillo [21] and Noon [5] included Lennard–Jones terms for the C–H pairs which increase the water–carbon binding energy. It can be seen that the Markovic [20] and Noon [5] potentials lead to complete wetting of the graphite surface, which indicates the potentials used to describe the water–graphite interaction are too strongly attractive. For the remaining five potentials, it is not possible to judge their accuracy unless a calibration criterion like matching the experimental contact angle is used. Using the higher target value [8–10] of 85 ± 2° for the macroscopic contact angle, the Walther *et al.* [22] potential has insufficient water–carbon attraction and the potentials of Gordillo and Marti [21] and Hummer *et al.* [3] are slightly too attractive. On the other hand, if Schrader's [11] lower target value of 42 ± 7° is used, the Gordillo and Marti and Hummer *et al.* potentials are more accurate. Unfortunately, it is not possible to completely rule out either of these experimental values for the macroscopic contact angle. Therefore, we consider the Gordillo and Marti, Hummer *et al.* and Werder *et al.* [6] potentials to have comparable accuracy. Based on the ΔE values, we expect the potential used by Koga [23] should also lead to contact angles in the target range. This will be discussed further in the "Results for the Discrete Model Potential" Section. In the present paper, the water–carbon potentials listed in Table I are called discrete models, because the graphite surface is described as a set of carbon atoms at positions given by the crystal structure of graphite.

For the present study, we also derived a new water–graphite interaction potential (called the continuum model). In some previous studies [26] of graphite and carbon nanotube interactions, the carbon surface has been represented by a continuous uniform sheet and the interaction of a test particle with the surface was calculated as a function of its normal distance above the surface (z). For a test particle over a single graphene layer, one can replace the discrete sum over Lennard–Jones terms for all carbon-test particle distances by a two-dimensional integral and obtain the following analytical potential:

$$V(z) = (2/5)\pi\varepsilon_{CO} D_C \sigma_{CO}\left[2(\sigma_{CO}^2/z)^{10} - 5(\sigma_{CO}/z)^4\right] \quad (5)$$

where σ_{CO} and ε_{CO} are the parameters from the original Lennard–Jones potential and D_C is the surface number density of carbon atoms (0.38 Å^{-2} for a single layer of graphite). The minimum of the continuum potential occurs at $z = \sigma_{CO}$ with $V(\sigma_{CO}) = -1.4326 \times \sigma_{CO}^2 \varepsilon_{CO}$. To construct a multilayer model of the graphite surface, the energy is given by

$$E(z) = V(z) + V(z + 3.4\,\text{Å}) + V(z + 2 \times 3.4\,\text{Å}) + \text{etc.} \quad (6)$$

There are two ways the continuum and discrete models differ: (1) the continuum potential

TABLE I Summary of published water–carbon interaction models*

Study	*Water model*	σ_{CO} (Å)	ε_{CO} (kJ/mol)	Δ (kJ/mol)	θ (°)
Markovic [20]	SPC†	3.190	0.3910	− 12.64	0.0
Gordillo and Marti [21]	SPC-FLX‡	3.280	0.3890	− 9.91	55.9
Walther [22]	SPC-FLX	3.190	0.3135	− 5.19	111.3
Hummer [3]	TIP4P¶	3.275	0.4785	− 8.12	48.0
Koga [23]	TIP4P	3.262	0.3876	− 6.53	
Noon [5]	TIP3P¶	3.296	0.5781	− 16.54	0.0
Werder [6]	SPC/E	3.190	0.392	− 6.33	95.3

* The Markovic [20], Gordillo [21] and Noon [5] models also included pairwise Lennard–Jones potential terms between carbon atoms and the water hydrogen atoms. † SPC is the original Simple Point Charge model for water [24]. ‡ SPC-FLX is a flexible water model that allows OH stretch and HOH bending motions (see Ref. [22]). ¶ TIP3P and TIP4P are rigid water models developed by Jorgensen and coworkers [25].

TABLE II Single water molecule-graphite binding energy (ΔE) in kJ/mol for the discrete surface model (dependence on binding site, number of layers and long-range cut-off for $\sigma_{CO} = 3.19$ Å and $\varepsilon_{CO} = 0.392$ kJ/mol)*

Cut-off (Å)	*No. of layers*	*ΔE (six-fold site)*	*ΔE (two-fold site)*	*ΔE (one-fold site)*	*ΔE (average)*	*ΔE (continuum)*
∞	2	− 6.522	− 6.213	− 6.177	− 6.271	
20	2	− 6.510	− 6.201	− 6.165	− 6.259	− 6.235
10	2	− 6.329	− 6.020	− 5.986	− 6.083	
20	8	− 6.645	− 6.331	− 6.295	− 6.392	
20	1	− 5.947	− 5.635	− 5.672	− 5.732	− 5.715

* Binding sites are described in the text; ΔE(average) is determined for seven binding sites.

completely neglects the surface corrugation effect and (2) in the continuum model, long-range truncation can only be applied in the normal direction. To examine these factors, the discrete potential model was evaluated for a single water molecule positioned over eight 210×245 Å graphene layers (staggered as in crystalline graphite with an interlayer spacing of 3.4 Å). The Lennard–Jones parameters recommended by WWJHK were used ($\sigma_{CO} = 3.19$ Å and $\varepsilon_{CO} = 0.392$ kJ/mol). Table II contains the computed binding energies (ΔE) for an SPC/E water molecule above several locations on this model graphite surface. The binding energy is the lowest value for V_{CO} in Eq. (1) as the distance between the water oxygen and the bonding site on the surface is varied. For these calculations, there is no interaction between the water hydrogens and the surface. For the six-fold site the water is directly over the center of a hexagonal ring, for the two-fold site it is over the center of a C–C bond and for the one-fold site it is directly over one of the carbon atoms. The ΔE (average) value corresponds to the unweighted sum of seven positions above the surface. All binding sites are located near the center of the top graphene layer so the effective truncation distance for the full summation is greater than 100 Å. It can be seen that the six-fold site has the strongest binding energy, about 0.25 kJ/mol lower than the average value. This is a measure of the magnitude of the surface corrugation. The second graphene layer contributes about 0.55 kJ/mol to the binding energy and the remaining six layers contribute only 0.15 kJ/mol, which demonstrates the soundness of using only two graphene layers in the MD simulations of WWJHK and in the present study. Finally one can see that using a cut-off of 20 Å results in only small changes in ΔE (~0.01 kJ/mol) compared to the full pairwise summation, but using a 10 Å cut-off results in errors of ~0.2 kJ/mol in the binding energy. The continuum model includes contributions from an infinite surface and the cut-off only applies to the normal distance to the water molecule. The original WWJHK study used a 10 Å cut-off and one would find a slightly different optimal ε_{CO} value if a larger cut-off distance was employed. Thus, we expect differences in the MD results when comparing the discrete and continuum models. For comparison, the discrete and continuum potentials for a water molecule over a single graphene layer are shown in Fig. 1. Note that all the potential curves shown are similar except for the six-fold case for which the energy minimum is deeper and occurs at 0.1 Å smaller z.

METHODOLOGY

Molecular dynamics simulations are carried out for a water droplet on a graphite surface to compute the contact angle as a function of the interaction strength of the water–carbon potential. Both the discrete and continuum graphite surface models described in the previous section are used. For the discrete model, the surface is modeled by two rigid 119×118 Å graphene sheets fixed in a parallel staggered configuration 3.4 Å apart. For the continuum model the graphite is represented by two planar layers each 200×200 Å with a fixed interlayer spacing of 3.4 Å. Periodic boundary conditions are used for the MD simulations with the computational box defined in two dimensions by the size of the graphite surface and 100 Å for the third dimension. Most simulations used a 2000-water droplet.

The extended Simple Point Charge water model SPC/E [12] used in this work has rigid water molecules with OH bond lengths of 1.0 Å and an H–O–H bond angle of 109.47°. Each oxygen atom has a partial charge of −0.8476e and each hydrogen atom has a partial charge of +0.4238e. The water–water interaction energy is the sum of the Coulomb energies between all pairs of point charges on different water molecules plus the sum of O–O Lennard–Jones energies with $\varepsilon_{OO} = 0.6502$ kJ/mol and $\sigma_{OO} = 3.166$ Å. The SPC/E water model reproduces experimental data for liquid water near ambient conditions, including the density, cohesive energy, dipole moment, viscosity and hydrogen bond populations. For simulations with the discrete surface model, the water–graphite interaction is described completely by the sum of pairwise Lennard–Jones energies as given by Eq. (1). In all cases, these terms are computed between water oxygen atoms and graphite carbon atoms, but for some of the cases the water hydrogen–carbon terms are also included. For simulations with

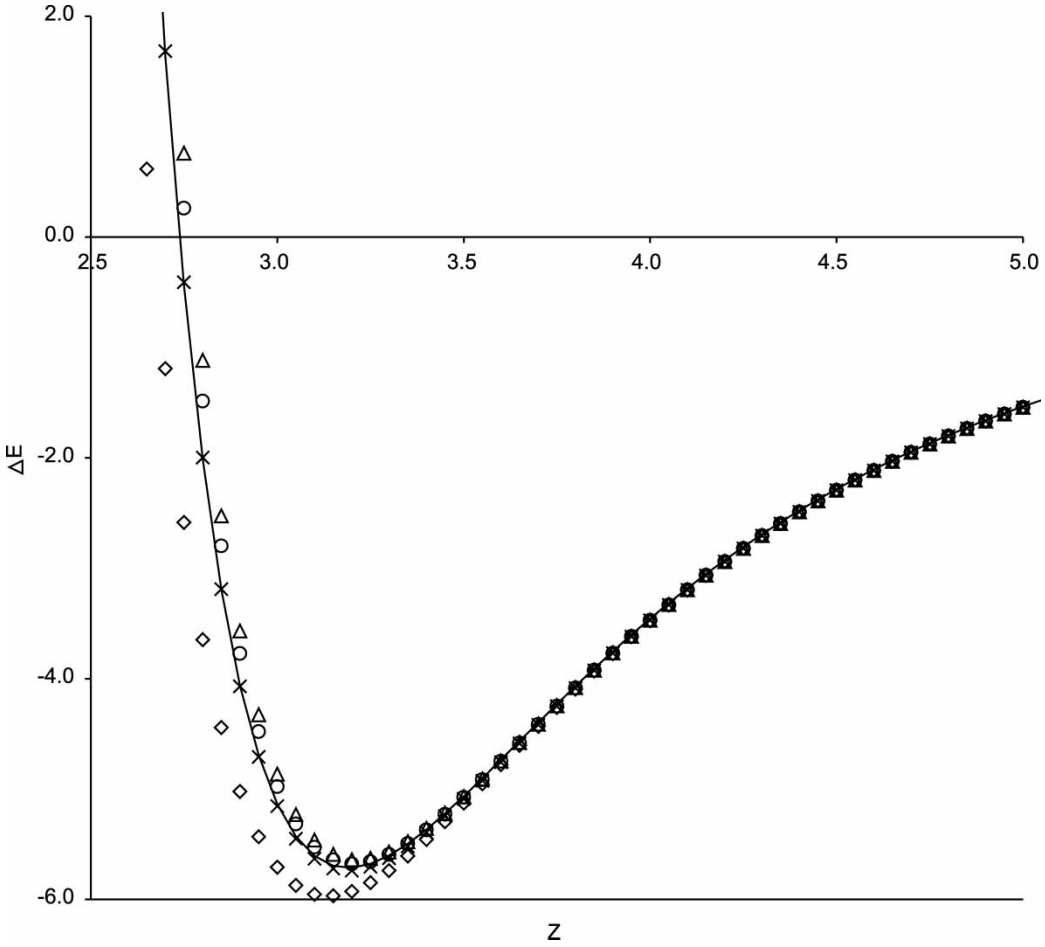

FIGURE 1 Interaction energy (ΔE) in kJ/mol for a single water molecule over a planar graphene sheet as a function of the height (in Å) of the water oxygen above the carbon surface as calculated using the discrete Lennard–Jones potential for $\sigma_{CO} = 3.19$ Å and $\varepsilon_{CO} = 0.392$ kJ/mol. Points are energies for the six-fold site (diamonds), two-fold site (circles), one-fold site (triangles) and average of seven locations on the surface (×). Solid line is calculated using the continuum model potential with the same parameters.

the continuum model, the water–graphite interaction is described by Eq. (6) as the sum of all water oxygen-surface energies.

The MD simulations in the present work are performed using the molecular dynamics code FASTTUBE [27]. These calculations were carried out as described by WWJHK. Each MD trajectory is 1 ns in length with 200 ps constant temperature equilibration at 300 K followed by an 800 ps constant energy simulation. Samples of the trajectory are stored at 0.2 ps intervals over the last 600 ps for data analysis. A time step of 2 fs is used. For each set of water–carbon parameters, we calculate the droplet base radius (r_B), the total water–graphite interaction energy (E_{CO}) and the static contact angle (θ) of the droplet using the procedures given by Werder *et al.* [6]. We normalize E_{CO} by dividing by r_B^2 to compare results for droplets with different numbers of water molecules. To compute the contact angle, the method of de Ruitjer *et al.* [28] is used. This involves decomposing the water droplet among cylindrical bins and generating isochore profiles. For each horizontal layer of bins an equimolar dividing surface (density = 0.5–0.8 g cm^{-3}) is determined and a circular fit to this surface is extrapolated to the graphite surface where θ is measured. Data from bins lying less than 8 Å from the graphite surface are not included in the circular fit because they are too noisy. Figure 2 illustrates this method for computing the contact angle and shows a snapshot of a typical droplet from the MD simulations.

RESULTS

MD simulations are carried out for the discrete and continuum graphite surface models described in the "Water–carbon Potential Models Section". Summaries of these results are given in Table III for the discrete model and in Table IV for the continuum model. The calibration curves of θ vs. ε_{CO} are shown in Figs. 3 and 4 for the discrete and continuum models, respectively. The entries in Table III with

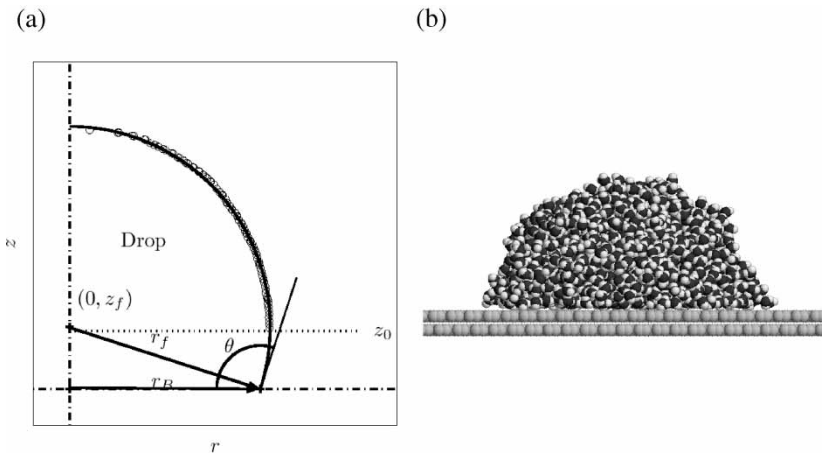

FIGURE 2 (a) Contact angle of a water droplet on graphite from MD simulations. The contact angle is measured by fitting a circle with center $(0, z_f)$ and radius r_f to the points of the equimolar dividing plane (circles) with $z > z_0 = 8$ Å to exclude the near wall region. The droplet has a base radius r_B. (b) Snapshot (at $t = 0.2$ ns) of a simulation at 300 K using the SPC/E water model, and a carbon–oxygen Lennard–Jones potential with parameters $\varepsilon_{CO} = 0.392$ kJ/mol and $\sigma_{CO} = 3.19$ Å. The two graphite layers are shown.

case numbers ending in W are data from Table II of WWJHK.

Results for the Discrete Model Potential

WWJHK used a series of discrete water–carbon potential parameters in their MD simulations that yielded behavior from hydrophobic ($\theta > 90°$) to completely wetting ($\theta = 0°$) They observed linear relationships between the binding energy of a single water molecule on graphite (ΔE) and the contact angle (θ) for a water droplet on graphite and between ΔE and the value of ε_{CO} in the water–carbon potential. Using the SPC/E water model with a long-range cut-off of 10 Å, their data show complete wetting for $\Delta E < -12.8$ kJ/mol. From these results, they could predict the binding energy for a water molecule on graphite that would yield a specific value of θ for the droplet and use that ΔE value to determine the optimal value for ε_{CO}. Their work represented a new method for calibration of molecular dynamics interaction potentials for molecular dynamics simulations and led to the recommended water–carbon Lennard–Jones parameters $\varepsilon_{CO} = 0.392$ kJ/mol and $\sigma_{CO} = 3.19$ Å that yield a binding energy of -6.33 kJ/mol for a single water molecule on graphite, a contact angle for a 2000-molecule water droplet of 95.3° and a macroscopic contact angle of $\theta_\infty = 86°$ (case 28W in Table III). In the present study, we have simplified this procedure by directly using the linear fit to the droplet contact angle as a function of ε_{CO} for calibration of the Lennard–Jones potential parameters. This calibration is illustrated in Fig. 3.

TABLE III Summary of MD simulations using the discrete water–carbon model potential

*Case**	σ_{CO} (Å)	ε_{CO} (kJ/mol)	σ_{CH} (Å)	ε_{CH} (kJ/mol)	*Cut-off* (Å)	r_B (Å)	*E*(CO) (kJ/mol)	ΔE (kJ/mol)	θ (degrees)
1	3.19	0.3651			10	27.52	− 1253.0	− 5.89	103.61
2	3.19	0.3651			12.5	29.91	− 1479.4	− 5.99	95.42
3	3.19	0.3651			15	30.63	− 1558.2	− 6.04	94.68
4	3.19	0.3651			17.5	31.07	− 1618.5	− 6.05	91.28
5	3.19	0.3651			20	30.64		− 6.06	92.37
10W	3.19	0.4389			10	32.80	− 2027.9	− 7.09	85.50
6	3.19	0.4389			20	38.21	− 2807.2	− 7.29	68.15
28W	3.19	0.392			10	30.10		− 6.33	95.30
7	3.2984	0.5346			10	46.13	− 4823.9	− 9.17	47.69
24W	3.275	0.4785			10	39.40		− 8.12	65.40
27W	3.296	0.4389			10	35.60		− 7.53	76.80
17W	3.19	0.2508			10	20.1		− 4.05	127.8
18W	3.19	0.3762			10	28.2		− 6.08	101.2
21W	3.19	0.627			10	58.00		− 10.13	29.40
22W	3.19	0.391	2.82	0.253	10			− 12.18	0
23W	3.28	0.389	2.81	0.129	10	42.40		− 9.70	55.90
25W	3.296	0.5781	2.58	0.323	10			− 16.54	0
8	3.19	0.2508	2.81	0.129	10			− 7.08	93.60
9	3.19	0.3135	2.82	0.202	10			− 9.88	57.60

* All cases are for 2000-water molecule droplets; Case numbers with W are data from Werder *et al.* [6].

TABLE IV Summary of MD simulations using the continuum water–carbon model potential

Case	σ_{CO} (Å)	ε_{CO} (kJ/mol)	#H_2O	*Cut-off (Å)*	r_B (Å)	E_{CO} (kJ/mol)	(θ) (degrees)
1	3.19	0.05	2000	10	0	− 13.0	180
2	3.19	0.1	2000	10	1.63	− 69.9	176.16
3	3.19	0.15	2000	10	13.29	− 170.8	147.30
4	3.19	0.2	2000	10	20.71	− 369.2	126.26
5	3.19	0.25	2000	10	22.11	− 601.1	121.71
6	3.19	0.3	2000	10	26.47	− 943.7	107.48
7	3.19	0.35	2000	10	29.24	− 1345.3	97.92
8	3.19	0.4	2000	10	31.85	− 1877.6	88.79
9	3.19	0.45	2000	10	36.36	− 2656.1	73.85
10	3.19	0.5	2000	10	40.52	− 3596.9	60.94
11	3.19	0.55	2000	10	48.68	− 5067.9	42.87
12	3.19	0.6	2000	10	61.76	− 7978.7	27.60
13	3.19	0.3651	1000	10	23.65	− 955.1	96.30
14	3.19	0.3651	4000	10	38.07	− 2414.2	93.91
15	3.19	0.3651	8000	10	48.54	− 3838.5	92.42
16	3.19	0.3651	2000	10	30.09	− 1503.3	94.88
17	3.19	0.3651	2000	12.5	29.98	− 1547.0	94.91
18	3.19	0.3651	2000	15	30.97		91.77
19	3.19	0.3651	2000	17.5	30.56		92.91
20	3.19	0.3651	2000	20	30.69		92.36
21	3.2984	0.5346	2000	10	56.75	− 6568.2	31.32
22	3.19	0.4389	2000	10	35.73	− 2490.2	75.57

The solid line in that figure is a linear least squares fit to the data for $\sigma_{CO} = 3.19$ Å and a cut-off distance of 10 Å.

In the present study, additional MD runs are obtained using the discrete model potential to study the effect of the long-range cut-off on the contact angle and the addition of a Lennard–Jones term between the water hydrogens and the graphite carbon atoms. The data for cases 1–5 in Table III illustrate the effect of varying the long-range cut-off on the base radius, contact angle, and average total C–O interaction energy as well as the single water binding energy. For a cut-off distance of 10 Å θ equals 103.6°, but it drops to 92.4° for a cut-off distance of 20 Å. The drop radius (r_B) and total CO interaction energy are also quite sensitive to the cut-off distance, but the water binding energy and the quantity E_{CO}/r_B^2 are not. From Table III it can be seen that most of the changes in these quantities occur when the cut-off is changed from 10 to 12.5 Å. For the purposes of carrying out simulations of carbon surfaces in contact with bulk water layers using the Lennard–Jones C–O potential, the choice of cut-off distance affects the choice of ε_{CO} that should be used. The WWJHK value of $\varepsilon_{CO} = 0.392$ kJ/mol was determined for a cut-off of 10 Å. Using the data in Table III for $\varepsilon_{CO} = 0.3651$ (case 5) and 0.4389 kJ/mol (case 6), we find, by extrapolation,

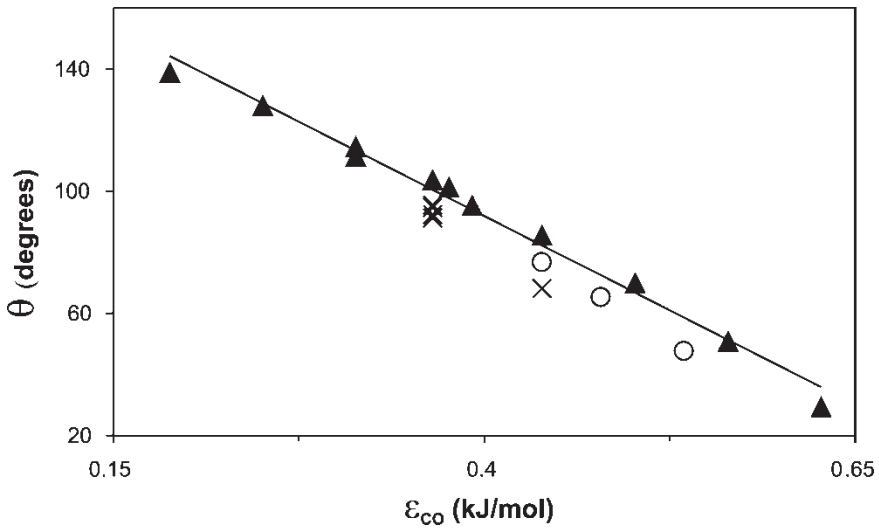

FIGURE 3 Computed contact angles for the discrete water–graphite model potential versus ε_{CO}. The triangles are data for cases with $\sigma_{CO} = 3.19$ Å and a cut-off distance of 10 Å from Table II of Werder *et al.* [6] and from Table III of the present work. The curve is a linear least squares fit to the subset of these data points ($\theta = 190.63° - 246.795\,\varepsilon_{CO}$). The points denoted by × are for cut-off distances greater than 10 Å. The unfilled circles are data for cases with $\sigma_{CO} \approx 3.29$ Å from Table III.

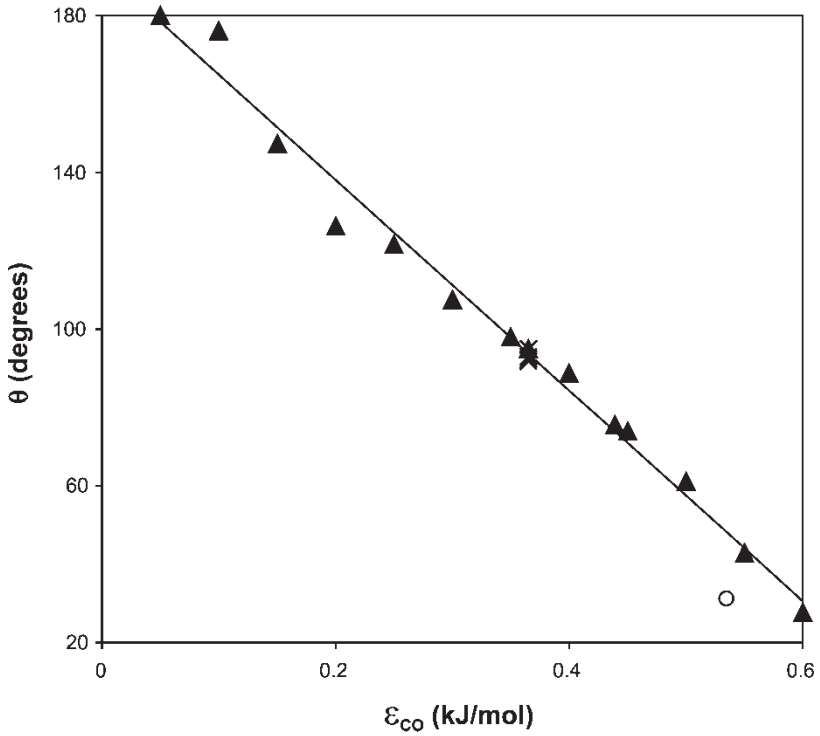

FIGURE 4 Computed contact angles for the continuum water–graphite model potential versus ε_{CO}. Triangles are from Table IV of the present work with $\sigma_{CO} = 3.19$ Å and a cut-off of 10 Å. The curve is a linear least squares fit to the subset of these data points ($\theta = 191.78° - 268.624\,\varepsilon_{CO}$). The points denoted by × are for cut-off distances greater than 10 Å. The unfilled circle is for the case with $\sigma_{CO} \approx 3.29$ Å.

$\varepsilon_{CO} = 0.357$ kJ/mol to be the optimum value for a 20 Å cut-off distance. This potential has a water binding energy $\Delta E = -5.93$, 0.4 kJ/mol smaller than the value determined for the 10 Å cut-off. The effect of varying the cut-off distance is also apparent in Fig. 3 where the triangles lying below the fitted line are data points that have been computed using cut-off distances larger than 10 Å.

The effect of including a C–H Lennard–Jones term in the potential is less clear. For a given ε_{CO} value, adding ε_{CH} increases the water–graphite binding and decreases the contact angle. However, the resulting contact angle is approximately 10° larger than if the same ΔE were achieved by increasing ε_{CO} (compare cases 8 and 10W or 9 and 21W in Table III). Clearly, adding the C–H Lennard–Jones term does not lower θ to the same extent that it increases the binding energy. For this model potential, the optimal water orientation has both OH bonds pointing toward the surface. In a droplet, however, the bottom layer of water molecules have at least one OH bond oriented parallel to the surface so it can form a hydrogen bond with other water molecules [22], thereby reducing the effective water–graphite binding energy. MD simulations using a discrete water–graphite potential with the C–H Lennard–Jones parameters of Gordillo *et al.* [21] ($\sigma_{CH} = 2.81$ Å and $\varepsilon_{CH} = 0.129$ kJ/mol) will match the target contact angle for $\varepsilon_{CO} = 0.2508$ kJ/mol, which is 34% smaller than the value recommended by WWJHK. Thus, when C–H Lennard–Jones terms contribute to the water–graphite interaction energy, those C–H terms contribute about 1/3 of the total water–graphite binding energy.

There is also limited data in Table III that illustrates the effect of changing σ_{CO}. The points represented by open circles in Fig. 3 are from MD simulations with $\sigma_{CO} = 3.29 \pm 0.01$ Å. It can be seen that increasing σ_{CO} by 0.1 Å decreases θ by 5–10° (compare cases 10W and 27W). For this larger value of σ_{CO}, we estimate that a value of 0.375 kJ/mol for ε_{CO} should be used to obtain the target contact angle of ~95°. This choice of parameters yields a water binding energy of −6.62 kJ/mol, which is 0.5 kJ/mol greater than case 18W in Table III (with $\sigma_{CO} = 3.19$ Å and $\varepsilon_{CO} = 0.3762$ kJ/mol) that has $\theta = 101.2°$ and $\Delta E = -6.08$ kJ/mol. The parameters used by Koga [23] as given in Table I ($\sigma_{CO} = 3.262$ Å and $\varepsilon_{CO} = 0.3876$ kJ/mol) are close to our estimate and yield a value of −6.53 kJ/mol for ΔE.

Finally, an additional MD run (case 7 in Table III) was carried out to illustrate the result of using the standard mixing rules for Lennard–Jones parameters (Eq. (2)). The original potential for carbon nanotubes and graphite used $\sigma_{CC} = 3.4309$ Å

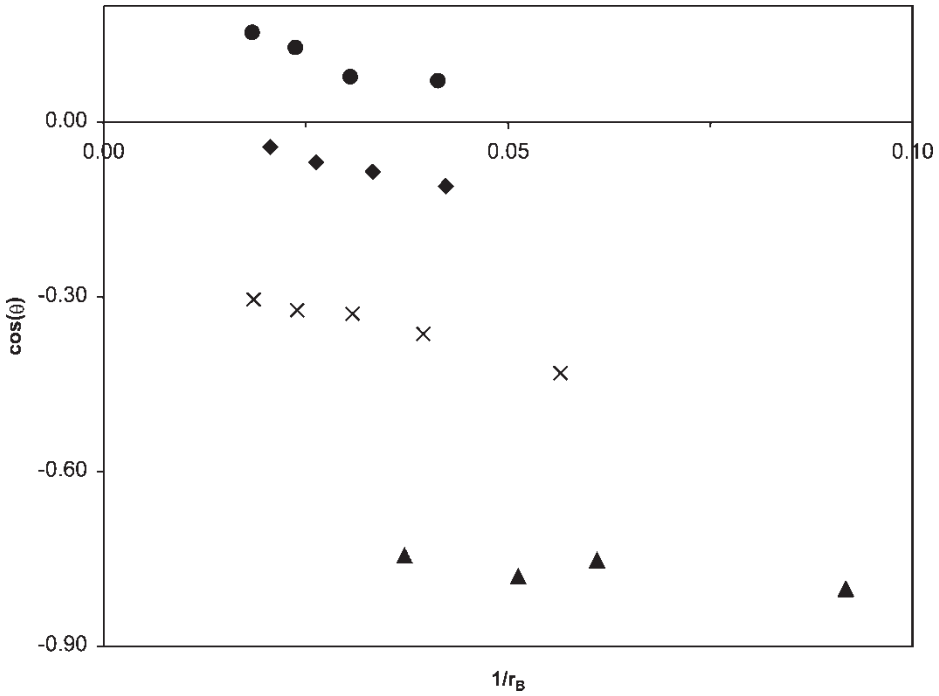

FIGURE 5 Cosine of the contact angle θ as a function of the droplet base curvature $1/r_B$. Points represented by diamonds are from the present study using the continuum graphite surface model ($\varepsilon_{CO} = 0.3651$ kJ/mol). The other three series of points are from Werder *et al.* [6] using the discrete graphite surface model with Lennard–Jones parameter $\varepsilon_{CO} = 0.1881$ kJ/mol (triangles), 0.3135 (×), 0.4389 (circles).

and $\varepsilon_{CC} = 0.4396$ kJ/mol. Combining these with the SPC/E O–O Lennard–Jones parameters ($\sigma_{OO} = 3.166$ Å and $\varepsilon_{OO} = 0.6502$ kJ/mol) yields $\sigma_{CO} = 3.2984$ Å and $\varepsilon_{CO} = 0.5346$ kJ/mol. Case 7 has a water binding energy of -9.17 kJ/mole and contact angle of 47.69°, which is considerably smaller than the recommended value of $\theta = 95.3°$ (case 28W).

Results for the Continuum Model Potential

For the continuum graphite surface model potential (Eq. (5)), we first systematically varied the Lennard–Jones well depth parameter ε_{CO} between 0.05 and 0.60 kJ/mol (cases 1–12 in Table IV) to generate a calibration curve of θ vs ε_{CO} as shown in Fig. 4 (the solid line in the figure is a linear least squares fit of the data with $\sigma_{CO} = 3.19$ Å and a cut-off distance of 10 Å). Using the same target value for the contact angle as in WWJHK, we obtain an optimal value of $\varepsilon_{CO} = 0.3651$ kJ/mol (case 13). For this potential, the water–graphite binding energy is -5.81 kJ/mol and complete wetting should occur for $\Delta E < -11.13$ kJ/mol. This series of MD simulations is carried out for a 2000-molecule water droplet with a long-range cut-off of 10 Å. Using the optimal value of ε_{CO}, two additional series of simulations were carried out: variation of droplet size (cases 13–15 in Table IV) for determination of the line tension based on the modified Young's equation (Eqs. (3) and (4)), and variation of the long-range cut-off (cases 16–20 in Table IV).

WWJHK demonstrated previously that the variation of droplet size and contact angle was described well by the modified Young's equation. Figure 5 shows the result of similar calculations carried out for 1000 to 8000-molecule water droplets and the WWJHK results. The continuum model potential with $\varepsilon_{CO} = 0.3651$ kJ/mol results in a line tension of 2.2×10^{-10} J/m which is 20% less than the value found by WWJHK for the discrete potential (case 10W). We also find $(\theta - \theta_\infty)$ for the 2000-water droplet is 5.8°, slightly less than the 7.9° found for the discrete potential with $\varepsilon_{CO} = 0.4389$ kJ/mol. Therefore, this recommended value of ε_{CO} for the continuum potential has a macroscopic contact angle (θ_∞) of 89.1°. The values for the line tension (τ) determined for both the discrete and continuum water–graphite potential models ($2–3 \times 10^{-10}$ J/m) are in agreement with the recent work of Mugele *et al.* [19] who used atomic force microscopy to image micron and sub micron sized droplets on solid substrates, and the MD simulations of Bresme and Quirke [29] who studied nanoparticles at liquid–liquid interfaces. A positive sign for τ means the contact angle decreases with increasing drop size.

The variation of contact angle with long-range cut-off distance is less than observed for the discrete potential. The change in θ between a cut-off of 10 and 20 Å is only 2.5° (from 94.88 to 92.36°). For the discrete potential, most of the cut-off effect arises from the influence of carbon atoms far from the binding site, which is largest when the water molecule is close to the surface. For the continuum

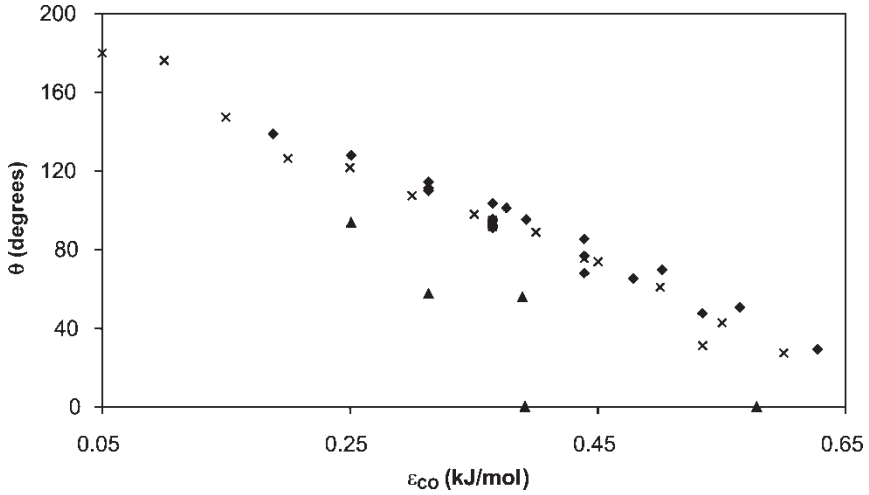

FIGURE 6 Calibration curve of contact angle as a function of ε_{CO}. The data for the discrete graphite surface model with only C–O Lennard–Jones energies are shown as diamonds, the data for the discrete model with C–O and C–H Lennard–Jones energies are shown as triangles, and the data for the continuum graphite surface model are denoted by ×. Data for the discrete models are from Table III of the present study and Table II of Werder *et al.* [6]. Data for the continuum model are from Table IV.

potential, the cut-off effect is entirely due to water molecules in the middle of the droplet and, therefore, farther from the surface. For this reason, calibration of the potential parameters is almost independent of the cut-off distance used in the MD simulations. Comparison of the computed contact angles using the discrete (with long-range cut-off of 20 Å) and continuum models shows that the discrete model leads to smaller contact angles for a given value of ε_{CO}. The difference in θ is 2.5° for $\varepsilon_{CO} = 0.3651$ kJ/mole and 7.4° for $\varepsilon_{CO} = 0.4389$ kJ/mole. When the 10 Å cut-off data points are used, the discrete model has contact angles that are 9–10° larger than the continuum model. For the most part, these differences in θ are attributable to differences in the water–graphite binding energy between the two models.

Comparison of Discrete and Continuum Models

A comparison of the calibration curves for the discrete and continuum graphite model potentials is shown in Fig. 6. It is noteworthy that the linearity of this relationship is apparent over the full range of contact angles between 30 and 180°. It can be seen that the continuum model data have slightly smaller contact angles than do the discrete data. The data for the discrete model that include the Lennard–Jones C–H potential are seen to lie on a substantially different curve. A linear relationship is also found

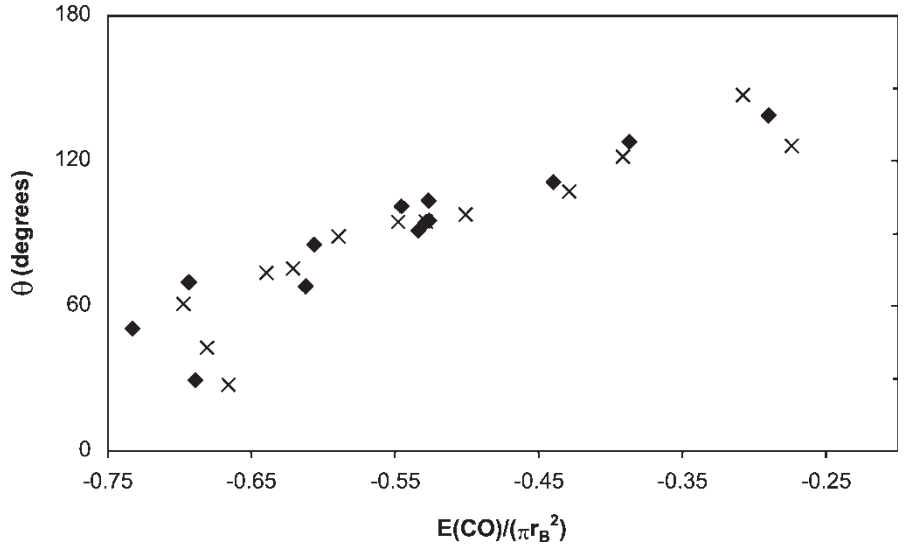

FIGURE 7 Contact angle as a function of the average total C–O interaction energy (E(CO)) divided by the base area of the droplet. The data for the discrete graphite surface model with only C–O Lennard–Jones energies are shown as diamonds and the data for the continuum graphite surface model are denoted by ×. Data for the discrete models are from Table III of the present study and Table II of Werder *et al.* [6]. Data for the continuum model are from Table IV.

TABLE V Summary of recommended parameters for water–graphite interaction energies

Model	σ_{CO} (Å)	ε_{CO} (kJ/mol)	σ_{CH} (Å)	ε_{CH} (kJ/mol)	*cut-off* (Å)	ΔE^* (kJ/mol)
Discrete	3.19	0.2508	2.81	0.129	10	− 7.08
Discrete	3.19	0.357			20	− 5.93
Discrete	3.29	0.375			10	− 6.62
Discrete†	3.19	0.392			10	− 6.33
Continuum	3.19	0.3651			10–20	− 5.81

*Based on the two-layer graphite surface model. †Recommended by Werder *et al.* [6].

between the contact angle and the average water–carbon energy, denoted E(CO), divided by the base area of the droplet, as shown in Fig. 7. The discrete and continuum models have similar behavior over the range $\sim 40° < \theta < \sim 150°$. Only data points at the extremes of this figure do not follow this relationship. It is likely that those values have larger errors due to more irregular droplet footprints on the surface, because the base area is computed from the average base radius assuming a circular profile. Finally, case 21 in Table IV for the continuum model, with $\theta = 31.32°$, corresponds to using the standard mixing rules for the C–O Lennard–Jones parameters. It should be compared with case 7 in Table III for the discrete model. For these parameters, switching from the discrete to continuum model results in lowering the contact angle by 16.4°. Both cases using the mixing rule parameters result in values for θ_∞ that are substantially smaller than any of the experimental values. Thus, we do not recommend the use of the standard mixing rule formulas for obtaining water–graphite Lennard–Jones parameters.

Table V lists the several recommended parameters for the water–graphite potential that can be used in MD simulations to reproduce the experimental macroscopic contact angle of 84–86° for water droplets on graphite. The entries are listed in order of increasing computational efficiency (e.g. discrete model before continuum one and longer cut-off distance before shorter one). Any of these parameter sets will yield contact angles of 92–95° for a 2000-molecule water droplet and macroscopic contact angles of 85–89°. These recommendations offer flexibility in setting the cut-off distance for truncation of the long-range Lennard–Jones potentials and in selecting the degree of detail for the water–graphite potential. They also illustrate how interrelationships between the various Lennard–Jones parameters influence the computed properties. It is evident, however, that ΔE should be in the range -5.8 to -7.1 kJ/mol.

CONCLUSIONS

In this paper, we have extended our previous calibration study [6] of potential energy functions used in MD simulations of water droplets on graphite surfaces. We use the contact angle of a 2000-molecule water droplet on a graphite surface because it arises from a balance between the water–water and water–graphite interactions and is sensitive to small changes in the parameters used in these potential models. In this work we have expanded upon the discrete graphite surface model used previously [6] by studying the effects of increasing the long-range cut-off for truncation of the Lennard–Jones terms and the effect of adding a Lennard–Jones term between water hydrogen and graphite carbon atoms. We have also studied a continuum graphite surface model based on the same C–O Lennard–Jones parameters.

We have computed the line tension by determining the change in contact angle with droplet size so we can extrapolate the contact angles for nanoscopic droplets to macroscopic ones. For the continuum graphite surface model presented in this study, the difference in contact angle between macroscopic and 2000-molecule size water droplets is 5.8°, similar to the value of 7.9° found by Werder *et al.* [6] for the discrete graphite surface model.

We studied the sensitivity of the contact angle to other factors in the simulation. The effect of varying the long-range cut-off of the Lennard–Jones potentials is minor for the continuum model, but sizeable for the discrete model. Switching from a cut-off of 10 to 20 Å reduces the contact angle by approximately 10° for the discrete model. The effect of adding a Lennard–Jones term between pairs of water hydrogen and graphite carbon atoms can be significant. However, if the water–graphite binding energy is kept nearly constant, the change in the contact angle is small.

Based on the MD simulations reported in this paper, we have five recommended parameter sets for the water–graphite interaction (presented in Table V). Use of these parameters in MD simulations of water–graphite interactions will result in macroscopic contact angles of 85–89° for water droplets on graphite surfaces. The data also demonstrate that the water–graphite binding energy is a qualitative indicator of the accuracy of the potential, because the recommended parameter sets yield values of $\Delta E = 6.50 \pm 0.65$ kJ/mol. All the parameter sets given in the Table are transferable to other carbon surfaces such as carbon nanotubes and fullerenes.

References

[1] Nguyen, C.V., Delzeit, L., Cassell, A.M., Li, J., Han, J. and Meyyappan, M. (2002) "Preparation of nucleic acid functionalized carbon nanotube arrays", *Nano Lett.* **2**, 1079.

[2] Li, J., Ng, H.T., Cassell, A., Fan, W., Chen, H., Ye, Q., Koehne, J., Han, J. and Meyyappan, M. (2003) "Carbon nanotube nanoelectrode array for ultrasensitive DNA detection", *Nano Lett.* **3**, 597.

[3] Hummer, G., Rasaiah, J.C. and Noworyta, J.P. (2001) "Water conduction through the hydrophobic channel of a carbon nanotube", *Nature* **414**, 188.

[4] Werder, T., Walther, J.H., Jaffe, R., Halicioglu, T., Noca, F. and Koumoutsakos, P. (2001) "Molecular dynamics simulation of contact angles of water droplets in carbon nanotubes", *Nano Lett.* **1**, 697.

[5] Noon, W.H., Ausman, K.D., Smalley, R.E. and Ma, J. (2002) "Helical ice-sheets inside carbon nanotubes in the physiological condition", *Chem. Phys. Lett.* **355**, 445.

[6] Werder, T., Walther, J.H., Jaffe, R.L., Halicioglu, T. and Koumoutsakos, P. (2003) "On the water–carbon interaction for use in MD simulations of graphite and carbon nanotubes", *J. Phys. Chem. B* **107**, 1345.

[7] Feller, D. and Jordan, K.D. (2000) "Estimating the strength of the water/single-layer graphite interaction", *J. Phys. Chem. A* **104**, 9971.

[8] Fowkes, F.M. and Harkins, W.D. (1940) "The state of monolayers adsorbed at the interface solid-aqueous solution", *J. Am. Chem. Soc.* **62**, 3377.

[9] Adamson, W. and Gast, A.P. (1997) *Physical Chemistry of Surfaces*, 6th Ed. (John Wiley and Sons, New York).

[10] Morcos, J. (1972) "Surface tension of stress-annealed pyrolitic graphite", *J. Chem. Phys.* **57**, 1801.

[11] Schrader, M.E. (1980) "Ultrahigh-vacuum techniques in the measurement of contact angles. 5. LEED study of the effect of structure on the wettability of graphite", *J. Phys. Chem.* **84**, 2774.

[12] Berendsen, H.J.C., Grigera, J.R. and Straatsma, T.P. (1987) "The missing term in effective pair potentials", *J. Phys. Chem.* **91**, 6269.

[13] Sorensen, R.A., Liau, W.B., Kesner, L. and Boyd, R.H. (1988) "Prediction of polymer crystal structures and properties: polyethylene and poly(oxymethylene)", *Macromol.* **21**, 200.

[14] Chen, J., Hamon, M.A., Yu, H., Chen, Y., Rao, A.M., Eklund, P.C. and Haddon, R.C. (1998) "Solution properties of single-walled carbon nanotubes", *Science* **282**, 95.

[15] Bojan, M.J. and Steele, W.A. (1987) "Interactions of diatomic molecules with graphite", *Langmuir* **3**, 1123.

[16] Courty, A., Mons, M., Dirnicoli, I., Piuzzi, F., Gaigeot, M.-P., Brenner, V., de Pujo, P. and Millie, P. (1998) "Quantum effects in the threshold photoionization and energetics of the benzene–H_2O and benzene–D_2O complexes: Experiment and simulation", *J. Phys. Chem. A* **102**, 6590.

[17] Feller, D. (1999) "Strength of the benzene–water hydrogen bond", *J. Phys. Chem. A* **103**, 7558.

[18] Jaffe, R.L. unpublished results.

[19] Mugele, F., Becker, T., Nokopoulos, R., Kohonen, M. and Herminghaus, S. (2002) "Capillarity at the nanoscale", *J. Adhesion Sci. Tech.* **16**, 951.

[20] Markovic, N., Andersson, P.U., Nagard, M.B. and Petterson, J.B. (1999) "Scattering of water from graphite: Simulations and experiments", *Chem. Phys.* **247**, 413.

[21] Gordillo, M.C. and Marti, J. (2000) "Hydrogen bond structure of liquid water confined in nanotubes", *Chem. Phys. Lett.* **329**, 341.

[22] Walther, J.H., Jaffe, R., Halicioglu, T. and Koumoutsakos, P. (2001) "Carbon nanotubes in water: Structural characteristics and energetics", *J. Phys. Chem. B* **105**, 9980.

[23] Koga, K., Gao, G.T., Tanaka, H. and Zeng, X.C. (2001) "Formation of ordered ice nanotubes inside carbon nanotubes", *Nature* **412**, 802.

[24] Berendsen, H.J.C., Postma, J.P.M., van Gunsteren, W.F. and Hermans, J. (1981) "Interaction models for water in relation to protein hydration", In: Pullman, B., ed, *Intermolecular Forces* (Reidel, Dordrecht), p 331.

[25] Jorgensen, W.L., Chandrasekhar, J., Madura, J.D., Impey, E.W. and Klein, M.L. (1983) "Comparison of simple potential functions for simulating liquid water", *J. Chem. Phys.* **79**, 926.

[26] Crowell, A.D. (1954) "Approximate method of evaluating lattice sums of r^{-n} for graphite", *J. Chem. Phys.* **22**, 1397.

[27] FASTTUBE: A parallelized Molecular Dynamics code written at the Institute of Computational Science, ETH Zurich by J.H. Walther, T. Werder and P. Koumoutsakos.

[28] de Ruitjer, M.J., Blake, T.D. and DeConnick, J. (1999) "Dynamic wetting studied by molecular modeling simulations of droplet spreading", *Langmuir* **15**, 7836.

[29] Bresme, F. and Quirke, N. (1999) "Nanoparticulates at liquid/liquid interfaces", *Phys. Chem. Chem. Phys.* **1**, 2149.